NREL/CP-500-25514

Validation of a Model for a Two-Bladed Flexible Rotor System: Progress to Date

Alan D. Wright, Neil D. Kelley,
Richard M. Osgood
National Wind Technology Center
National Renewable Energy Laboratory

Presented at
AIAA/ASME Wind Energy Symposium
Reno, Nevada
January 11- 14, 1999

National Renewable Energy Laboratory
1617 Cole Boulevard
Golden, Colorado 80401-3393
A national laboratory of the U.S. Department of Energy
Managed by Midwest Research Institute
for the U.S. Department of Energy
under contract No. DE-AC36-83CH10093

Work performed under task number WE901210

November 1998

NOTICE

This report was prepared as an account of work sponsored by an agency of the United States government. Neither the United States government nor any agency thereof, nor any of their employees, makes any warranty, express or implied, or assumes any legal liability or responsibility for the accuracy, completeness, or usefulness of any information, apparatus, product, or process disclosed, or represents that its use would not infringe privately owned rights. Reference herein to any specific commercial product, process, or service by trade name, trademark, manufacturer, or otherwise does not necessarily constitute or imply its endorsement, recommendation, or favoring by the United States government or any agency thereof. The views and opinions of authors expressed herein do not necessarily state or reflect those of the United States government or any agency thereof.

Available to DOE and DOE contractors from:
Office of Scientific and Technical Information (OSTI)
P.O. Box 62
Oak Ridge, TN 37831
Prices available by calling (423) 576-8401

Available to the public from:
National Technical Information Service (NTIS)
U.S. Department of Commerce
5285 Port Royal Road
Springfield, VA 22161
(703) 487-4650

Printed on paper containing at least 50% wastepaper, including 20% postconsumer waste

AIAA-98-0060

VALIDATION OF A MODEL FOR A TWO-BLADED FLEXIBLE ROTOR SYSTEM: PROGRESS TO DATE

Alan D. Wright
Senior Engineer
Neil D. Kelley
Principal Scientist
Richard M. Osgood
Senior Test Engineer

National Renewable Energy Laboratory
Golden, Colorado

ABSTRACT

At the National Renewable Energy Laboratory*, we tested a very flexible wind turbine. This machine, the Cannon Wind Eagle turbine, exhibited an ability to significantly reduce the rotor flap-wise bending moments through a unique combination of a flexible rotor and hub design. In parallel to this testing effort, we developed analytical models of this machine using our simulation codes.

The goal of this work was to validate the analytical models of this machine by comparing analytical predictions to measured results from the real machine. We first describe briefly the simulation codes used in this study. We then describe the wind turbine we analyzed. We then describe analytical model validation progress for this flexible rotor and show preliminary validation results. Finally, we make conclusions and state our plans for future studies.

INTRODUCTION

Designing long-lasting, fatigue-resistant wind turbines at minimal cost is a major goal of the U.S. Wind Energy Program and the wind industry. To achieve this goal, we must be able to design wind turbines that exhibit reduced loads compared to current machines. One possible method for reducing structural loads in wind turbines is to design machines with very flexible components. A challenge in designing flexible machines is to design the machine to avoid unwanted vibration and resonance problems. We must have well validated structural dynamic models in order to design these machines to meet these criteria.

Some validation of a flexible wind turbine model was performed by Garrad Hassan & Partners Ltd.[1] They validated the BLADED code for an earlier version of the machine that we tested at the National Wind Technology Center (NWTC). BLADED uses a modal approach for representing the elastic degrees of freedom. They found that the modal approach of representing the blade and tower elastic degrees of freedom was reliable for predicting the overall fatigue behavior of this type of wind turbine. They also found that in stalled flow conditions, the predicted loads exhibited larger dynamic variation than were present in the measurements. They went on to conclude that this discrepancy was most likely due to an underprediction of the extent of aeroelastic damping in the model. They concluded that this was due to the modeling of unsteady aerodynamic stall on a rotating wind turbine blade and was not specific to the flexible, lightweight configuration of this type of turbine.

At the National Renewable Energy Laboratory (NREL), we modeled this type of flexible wind turbine using the Automatic Dynamic Analysis of Mechanical Systems (ADAMS†) software to calculate dynamic loads and response of wind turbines. Unlike codes using a modal method of representing the elastic

* This paper is declared a work of the U.S. Government and is not subject to copyright protection in the United States.

† ADAMS is a registered trademark of Mechanical Dynamics, Inc.

degrees of freedom in a wind turbine, the ADAMS code divides the flexible components into a series of rigid body masses. These masses are then connected together with elastic elements. We then use the University of Utah AeroDyn aerodynamic subroutine package to supply the aerodynamic forces to ADAMS.[2] A further description of this modeling effort for this machine can be found in a paper by Wright. [3]

In this paper we describe analytical model validation progress for this flexible system. We show code validation results for this machine, using the ADAMS software. We show validation results from ADAMS by comparing model predictions to measured data for a few important operating conditions. One goal of our work is to show the accuracy of predictions from an "initial" model of this machine, before any comparisons with measured loads have been performed. We developed an "initial" model (Model-1) of the turbine using input properties obtained from manufacturer's drawings and specifications. We did not tune the input properties of this model, except to adjust the rotor blade lag stiffness values, which we felt were too low. We also show comparisons from a "tuned" model (Model-2), in which turbine property input was refined in order to obtain close agreement between measured and predicted turbine natural frequencies.

We began our validation with comparisons of predicted natural frequencies to measured results for the isolated blade flexbeam and shell. We then compared predicted modal responses to measurements taken from the complete wind turbine system, with the rotor parked. We then performed comparisons of predicted loads to measured field data. After completing the validation, we drew conclusions and identified future goals, which are presented at the end of the paper.

TURBINE DESCRIPTION

The machine modeled in this study is the Cannon Wind Eagle 300 (CWE-300) machine. The CWE-300 machine is a flexible, lightweight, wind turbine design that uses two blades mounted downwind of a guyed, tilt-up tower. The machine consists of three primary mechanical subsystems: a rotor, a nacelle, and a tower.

The Wind Eagle rotor consists of two identical blade shells attached to a central flexbeam spar. Figure 1 shows a diagram of the rotor. The flexbeam and the blade shells are constructed of vacuum-bagged, E-glass/epoxy composite and are designed for high flexibility in the flap-wise direction. The blade shells are constructed from three main components and several smaller parts, which are bonded together during final assembly. An aluminum rib forms the root end of the blade shell.

The flexbeam is continuous across the hub and is clamped to the hub center. The blade shells are connected to each end of the flexbeam through a spherical joint. Each tip of the flexbeam is attached inside of each blade shell at approximately 2.4 meters (m) outboard of the shell root rib.

The blade shell root rib serves as a hard attachment point for the blade arm and the pitch-pivot rod bracket. Those two components connect the blade shell to the pitch assembly and the rotor hub. The blade shell pitch-pivot rod fits into the pitch-pivot bearing mounted on the hub. The pitch-pivot rod can slide in and out of the pivot bearing, as well as rotate about an axis roughly parallel to the blade centerline. The blade can be pitched approximately 20 ° about this bearing.

The Cannon Wind Eagle hub mechanism uses a central yoke to provide collective pitching for both blades simultaneously. Aerodynamic stall is used to regulate power during normal operation, unlike the pitch-to-feather approach used in conventional pitch control turbines. The CWE-300 blades are pitched deep into stall during turbine shutdown, providing rotor stops in normal and emergency situations. Mechanical braking is unnecessary except to park the rotor. The blade shell root rib is connected to the pitch linkage by a spherical joint. The pitch link is attached to the pitch beam through a revolute joint.

The nacelle of the CWE-300 attaches to the tower by a yaw bearing and is free to rotate 360° about the yaw axis. A hydraulic yaw drive system is used to aid rotor tracking and also can be activated to manually yaw the machine for maintenance purposes. The nacelle mainframe is mounted with a linear damper and trunnion arrangement, allowing nacelle tilt over a limited range (plus and minus 5 °). Damping can be added to both the yaw and tilting DOF, and the tilting range can be adjusted by replacing the rubber tilt bumpers. The nacelle is supported on a guyed, tubular tower that can be tilted for installation and maintenance.

MODELING DESCRIPTION

All of the properties, which were necessary to prepare an analytical model of the machine, were summarized in a report prepared by Dynamic Design. [4] They reviewed machine drawings and summarized all of the properties into tabular form. After careful review of these properties, we developed a model of the tower, nacelle, and drive train using ADAMS/WT. [5] We modeled the tower as an Euler beam by dividing

the tower into eight lumped masses and then connecting them together with elastic beam elements. The base of the tower is attached to the ground with a revolute joint, which simulates the actual pin connection for raising and lowering the tower for maintenance purposes. We also included simple linear elastic guy wire effects as linear spring-dampers, with the stiffness coefficients determined from the guy wire diameter and material.

We attached the nacelle to the tower in such a way as to allow both yaw and tilt degrees of freedom (DOF). We added nacelle soft-tilt stops engaging at plus and minus 5° of nacelle tilt. At 6° of nacelle tilt, the nacelle reached hard-stop limits (which have stiffness values about 100 times the soft stop values). We set the tilt stiffness and damping to values given to us by the manufacturer for tilt angles between the stop limits.

We incorporated a torsion degree of freedom into the drive train by modeling the low-speed shaft as two lumped masses (PARTS) connected by a torsional spring. We assigned the torsional spring a value from an analysis of the low-speed shaft dimensions and material constants. We neglected drive train shaft bending, because we felt that the most important modes of the turbine were predicted quite well without this degree of freedom, and we wanted to reduce the complexity of our models. We neglected gearbox effects as well as the high-speed shaft. We incorporated a very crude generator model using an equation that applies a generator force directly to the low-speed shaft.

We then developed a simple model of the hub and connected it to the end of the low-speed shaft with a rigid connection. We then developed a model of the flexbeam. We obtained estimates of the distributed mass and stiffness of this component and then used ADAMS/WT to produce the ADAMS model. The flexbeam was modeled as an Euler Beam by dividing it into a series of rigid body parts connected by beam elements (we actually used the ADAMS FIELD statements as generated by ADAMS/WT). For this model we used ten rigid body parts connected by nine FIELD statements for the entire spar. We then connected the center of the flexbeam to the hub with a fixed joint (allowing no relative motion between the hub and flexbeam).

The blade shell was modeled similarly, using 15 rigid body parts and beam elements per shell. We attached aerodynamic markers to each part to represent the aerodynamic forces. We modeled the large amount of pre-twist (approximately 36° at the root of the shell). Each identical blade shell was then connected to each end of the flexbeam using a spherical joint connection, which allowed transmission of tension and shear forces from the shell to the flexbeam, but excluded bending moments. We did not connect the blade shell to the flexbeam at the shell root rib. Instead we connected it to the flexbeam at a point on the shell located well outboard of the root rib. This replicated as closely as possible the exact attachment location of the shell to the flexbeam in the real machine. Figure 2 shows an illustration of our ADAMS model of this rotor.

We also modeled the pitch-pivot bearing connecting the shell root rib to the hub. We modeled this connection in ADAMS with a spherical joint and a cylindrical joint. The spherical joint allowed rotation of the ball, which is imbedded in the hub, in any direction relative to the hub. We then connected the blade root rib with its pivot rod into this ball with a cylindrical joint, allowing rotation and translation of the pivot-rod relative to the ball.

We also developed a simple model of the blade pitch mechanism, using links and hinges. We did not model the pitch hydraulic mechanism. We simply fixed the pitch at the run position (4° toward feather as referenced to the blade tip). We felt it was important to model the connection of the blade root rib to the hub via the pitch pivot bearing and to the pitch link in order to simulate the correct boundary conditions. This blade exhibits significant coupling between elastic flap motion and blade rigid body pitch motion due to these boundary conditions. When the blade flaps downwind, the entire blade pitches toward stall.

Another coupling effect that exists in this blade is the coupling between blade elastic flap and elastic torsion, due to the location of the mass and elastic axis locations in the chordwise direction at each radial station along the blade. The blades of this machine contain significant ballast weights outboard near the blade's tip, located close to the leading edge. This ballast shifts the center of gravity of the blades from the centroid of the blade section to the leading edge, causing coupling between elastic flap and elastic torsion. The amount of coupling remains unknown, due to our lack of knowledge of the precise properties of these blades.

In all of these cases, we used the University of Utah AeroDyn subroutine package to generate the aerodynamic forces for the turbine rotor. We used version 10.0 of AeroDyn for all of these studies. For all of the results reported in this paper, the Beddoes dynamic stall model was turned on as well as the Pitt and Peter's Dynamic inflow model.

MODEL VALIDATION RESULTS

Since the model of this flexible wind turbine system was composed of a number of individual components, we felt that it was important to validate some of the separate components of this system, before assembly of the complete system model. We wanted to verify that our individual models had the correct mass and stiffness properties. We first performed individual modal tests of the isolated flexbeam and the isolated blade shell. We calculated the natural frequencies of these individual components without any aerodynamic loads. We then compared our predicted natural frequencies from our ADAMS models of these individual components to measured values.

We then validated our model of the complete turbine with the rotor parked, by comparing predicted natural frequencies to measurements for the complete turbine. The turbine was modal tested with the rotor parked (non-rotating) and we again excluded aerodynamic loads in these models.

We then went on to compare operating loads data to model predictions. In these models we included aerodynamic loads of the rotor. We now describe these validation steps. For an in-depth description of the instrumentation and data collection for this machine, see Kelley.[6]

Table 1. Comparison between Predicted and Measured Flexbeam Natural Frequencies

Mode Description	*Predicted Frequency Without Tip Mass (Hz)*	*Predicted Frequency With Tip Mass (Hz)*	*Experimental Frequency (Hz)*
1st Flap (S)	**7.48**	**6.12**	**5.99**
2nd Flap (A)	**15.77**	**12.79**	**13.30**
3rd Flap (S)	**28.08**	**23.58**	**25.33**
1st Torsion	**48.35**	**48.04**	**51.35**
1st Lag (S)	**55.54**	**45.31**	**44.75**

Table 2. Comparison of Predicted and Measured Blade Shell Natural Frequencies

Mode Description	*Predicted Frequency –Unrefined Inputs (Hz)*	*Predicted Frequency using Refined Lag Stiffness Inputs (Hz)*	*Modal Test (Hz)*
1st Flap	**1.39**	**1.50**	**1.68**
2nd Flap	**3.60**	**3.79**	**3.72**
1st Lag	**3.83**	**7.41**	**7.36**
2nd Lag	**10.06**	**20.00**	**21.32**
1st Torsion	**18.21**	**18.43**	**16.87**

Component Model Validation

We first performed a test of the flexbeam in order to determine experimentally its natural frequencies and mode shapes. It was not possible to clamp the flex-beam to a test stand, so we suspended the flexbeam from a laboratory ceiling using very lightweight cords. This setup simulated the flexbeam in a configuration having free-free boundary conditions.

In parallel, we modeled the isolated flexbeam using ADAMS. We then linearized this model and obtained predictions of the first few natural frequencies of the flexbeam. Table 1 shows a comparison of predicted and measured frequencies for various modes of the flex-beam. We found that it was important to include the mass at the tip of the flexbeam, which represents the spherical joint and attachment fittings. In general we found quite good agreement between measured and predicted natural frequencies which gave us confidence in our analytical model of the flexbeam.

Next, we performed a similar test for the blade shell. This component was suspended in the same manner as the flexbeam and a modal test was performed to determine the first several modes of vibration of the shell in the free-free configuration. We also modeled this isolated component with ADAMS and then linearized this model in order to determine its frequencies in the free-free configuration.

We see a comparison of these results in Table 2 for a few of the most important modes of the blade shell. We show two different sets of predictions in this table. When we first developed the shell model, using property data from Dynamic Design, we found that the discrepancy between measured and predicted lag frequencies was large, as seen in the table in column 2. In order to produce a model with more realistic lag natural frequencies, we simply increased the lag stiffness values by a factor of 10 (multiplied the lag stiffness by 10). The resulting natural frequencies produced by this revised model can be seen in column 3 of Table 2.

We observed significant coupling between the shell's flap, lag, and torsion degrees of freedom in all modes shown in Table 2. Even the first flap mode exhibited significant coupling between elastic flap and elastic torsion, due to the chordwise location of the center of gravity and elastic axis of the shell. We have not performed a rigorous comparison of the precise amount of twist/flap coupling between measurements and model predictions. We simply observed this coupling in the animation of various modes, both from our model predictions and the measured results.

We then used this revised shell model (the model with increased lag stiffness) in our ADAMS model of the full system. We call this model Model-1 (the "initial" model). We then compared predicted modal natural frequencies to measured modal results for the full system from this model.

Full System Model Validation

We first compared predicted natural frequencies of the full turbine to measured modal data. A modal test of the complete wind turbine system was performed with the rotor parked so that the blades were oriented vertically. We predicted the natural frequencies and mode shapes of the complete non-rotating turbine.

Table 3. Comparison of Measured and Predicted Turbine Natural Frequencies

Mode	*Measured Frequency (Hz)*	*Predicted Frequency Model-1 (Hz)*	*Predicted Frequency Model-2 (Hz)*
Rotor First Symmetric Flap	**0.45**	**0.32**	**0.44**
Rotor First Asymmetric Lag	**0.83**	**1.02**	**0.85**
Tower First Fore- Aft Bending	**0.92**	**0.85**	**0.95**
Tower First Side-Side	**1.02**	**0.79**	**1.07**
Rotor First Asymmetric Flap	**1.28**	**1.55**	**1.95**
Rotor Second Symmetric Flap	**1.61**	**1.36**	**2.12**
Rotor First Symmetric Lag	**2.38**	**2.02**	**2.39**

Table 3 shows this comparison. The full system initial ADAMS model (Model-1) seems to underpredict the rotor first symmetric flap mode by about 30%. We do not know the exact cause of this discrepancy. We think that this large discrepancy might be caused by friction and damping in the joints which connect the blade shell to the hub and pitch system. In Model-1 we have set all damping in these joints to zero.

Other predicted modal frequencies from Model-1 are "in the ballpark" compared to measured results. We have noticed that the measured rotor first asymmetric lag mode really involves extensive drive-train torsion (at 0.83 hertz [Hz]). Model-1 tends to overpredict this mode, because our initial estimate of the torsional stiffness of the low-speed shaft is too high.

The predicted tower fore-aft and side-side frequencies tend to be underpredicted, due to underestimated tower stiffness values. We later discovered that the real tower is composed of overlapping tower sections, causing larger stiffness in certain portions of the tower than we are using in our model.

In an effort to discover what changes in our model were necessary to obtain better predictions of these natural frequencies, we produced a second model (Model-2). We adjusted the tower stiffness and the low-speed shaft torsional stiffness in our original model to produce this "tuned" model (Model-2). We moved the tower first fore-aft and side-to-side bending frequencies from 0.85 Hz and 0.79 Hz to 0.95 Hz and 1.06 Hz respectively, by adding stiffness to the upper tower sections. In addition, we lowered the first drive-train torsional frequency from 1.02 Hz to 0.84 Hz by decreasing the torsional spring constant in our model.

We also added a large amount of damping in the pitch rod links and the spherical joints that connect the pitch links to the blade root rib. This damping raised the first symmetric flap mode from 0.32 Hz to 0.45 Hz.

The predicted natural frequencies from the tuned model (Model-2) are shown in column 4 of Table 3. Now the first symmetric flap mode is closer to the measured results. The second symmetric flap mode is over-predicted by Model-2 compared to measured data (2.12 Hz versus 1.61 Hz). The prediction of precise values of the first and second symmetric flap modes for this machine seems problematic. It seems like these modes are sensitive to the amount of damping that we incorporated into the pitch links and joints which connect the pitch rods to the blade root rib.

Next we compare predicted operating loads to measurements from both the "initial" model (Model-1) and the "tuned" mode (Model-2). In this study, we validated our model only for steady wind inflow conditions, omitting the effects of turbulent winds. We selected numerous short subsets of data, approximately 20 seconds in duration having steady winds and small yaw rates. The data was sampled at 200 Hz. Thus even a twenty-second data set contained about 4000 data points. We analyzed these data sets with the GPP postprocessor in order to obtain statistics of the data.[7] We also performed bin azimuth averaging of some of the load measurements, such as the flexbeam flap-wise and edgewise bending moments and the low-speed shaft torque.

Table 4. Characteristics of Some of the Validation Data Sets

Case	Mean Hub U_H (m/s)	s_H (m/s)	Mean Wind Direction (deg)	Vertical Shear (power law shear coefficient)	Mean Vertical wind speed (m/s)
dc01_s2	7.07	0.25	260.40	0.038	-0.54
dc05_s4	10.08	0.88	303.38	0.052	0.01
dc05_s1	13.79	1.35	300.03	0.062	0.67
dc12_s2	19.20	1.16	282.96	0.087	-0.71

We input an average power law shear profile as well as mean vertical wind speed from measured data into the model. We also input a tower shadow with a width of 2.04 m with a velocity deficit of 30%. We then

input constant winds to the model and ran the model for 40 seconds to assure a steady state trim solution.

We noticed that at low wind speeds, the real machine exhibited a higher yaw error than the model predicted, possibly due to rotor imbalance or other effects. We felt that the model would tend to overpredict the mean loads and power. We therefore decided to lock the yaw in our model and input a yaw error equal to the mean yaw error in the data for that data set.

Table 4 shows some of the statistics of the measured data for a few noted data sets that we used for our comparisons. Each case had quite a small vertical power law wind shear coefficient, while the mean vertical wind speed was significant in most cases.

Figure 3 shows a comparison of predicted and measured machine power for Model-1. In general, the power is reasonably well predicted over a range of wind-speeds up to about 16 m/s, beyond which the model tends to overpredict the power. This discrepancy could possibly be due to some error in the coupling between elastic flap motion and either blade rigid body pitch motion or elastic twist motion (caused by blade section mass, elastic axis, and aerodynamic center offsets). This discrepancy is being investigated further. We do not have accurate values of the sectional positions of the blade mass, elastic axis and aerodynamic centers for this blade. The discrepancy could also be due to the aerodynamic stall model.

We also compare the blade mean flexbeam flap-wise bending moments in Figure 4. These loads were measured on the flexbeam near the root. We see in this figure that the best correlation between predicted and measured loads occurs for Blade B. For this blade (lower portion of the figure) we see again that the model correlates well with the measured results at low to moderate wind speeds. For higher wind speed cases, the model tends to underpredict the mean flap-wise bending moments. For Blade A, the model tends to under-predict the bending moments over the entire range of wind speeds.

We show a comparison of the mean edgewise bending moments at the flex-beam in Figure 5. The best correlation between measured and predicted loads occurs for Blade B, with the model tending to over-predict the mean edge-wise bending moments as the wind speed increases. For Blade A, the model tends to underpredict the loads over the whole range of wind speeds.

We show azimuth averaged blade mean flap-wise and edge-wise bending moments for four different cases in Figures 6 and 7, for the cases tabulated in Table 4. In general the predicted responses agree well with the measured ones, except for the higher wind speed cases. In these figures we have shown results from both Model-1 and Model-2 (the "initial" and "tuned" models). We found that tuning our model to match the measured turbine modal data did not greatly change these results. Both models tend to predict about the same bending moments, with Model-2 tending to produce more highly damped results than Model-1.

Parametric Investigations

Through our analysis of the measured machine response, we noticed a large once-per-revolution (1P) variation in the machine power and low-speed shaft torque. In addition, we observed a large difference in mean loads between Blades A and B as seen in the measurements presented in Figures 4 and 5.

We are currently investigating various possible causes of these anomalies seen in the machine's behavior. Recently, we measured the weights and center of gravity locations of both blade shells and found that the weights of both blades were nearly identical. We also measured the center of gravity of both blade shells and found that there was a slight difference of about .024 m (1 inch). We decided to incorporate a small center of gravity difference between Blade A and Blade B of this magnitude by adding a small amount of mass inboard on Blade A. We made this modification to Model-2, because we felt that it was important for the natural frequencies of the modeled turbine to be close to those of the actual machine.

We then ran this model with the mass imbalance for all the cases delineated in Table 4. Figure 8 shows the results for one of our cases; the other cases produced similar trends to this case and are not shown. We show original "tuned" model (Model-2) results without any mass imbalance as well as results from the model with an imbalance in the lower portion of Figure 8. This figure shows the large 1P variation in the measured torque as well as predictions from the model with a mass imbalance. We also see that Model-2 results without the mass imbalance do not contain this 1P variation in the torque, even though the modes of the modeled parked turbine are close to those of the actual parked machine. This study indicates that the proximity of turbine natural frequencies to the rotor rotation frequency may not play a big role in this behavior. We needed to add a mass imbalance in order

to obtain a large enough variation in the rotor torque to be comparable to the measured results.

We found, however, that the "tuned" model with the addition of the mass imbalance did not predict the large difference in mean loads between Blade A and Blade B as we observed in the measured data.

We investigated other types of blade dissimilarities, such as blade pitch and twist differences. From observation of the mean flap-wise and edge-wise bending moments, it appears that Blade A has higher angles of attack than Blade B, because the mean moments are higher on Blade A than on Blade B. Another model that we exercised was a model with a twist difference between the two blades. This model was produced from Model-2 by re-orienting the aerodynamic markers of Blade A over the outer 30% of the blade so that they were oriented 2° toward stall, compared to those of Blade B. We show the resulting predictions of the low-speed shaft torque from this model in Figure 8 (upper plot). We see in this figure that this model predicts a large 1P variation in torque, even though the predictions are not in phase with the measured results. In addition, we found that this model predicts a large difference in the flexbeam mean edge-wise bending moments between the two blades, unlike the model with the mass imbalance. We have tried other types of blade dissimilarities, such as a pitch difference between Blade A and B and have found that these models predict similar behavior to the twist difference.

We currently do not know the exact cause of the difference between the measured loads between Blades A and B, or the 1P contribution in the machine power and low-speed shaft torque. Because the mean loads on one blade are different than on the other, we feel that there is a significant difference in the aerodynamic loads, which occur on one blade compared to the other. This difference could be due to simply different blade pitch settings, or it could be due to a difference in the twist distribution between the two blades as we have here demonstrated. We feel that this flexible turbine is very sensitive to small differences in the blades, as we saw when we incorporated a small mass imbalance in the rotor.

We are considering other possible explanations for this anomaly, such as a difference in the pitch/flap or flap/twist behavior of one blade versus the other. Perhaps Blade A has different coupled flap/twist characteristics than Blade B, resulting in a different pitch or elastic twist behavior and thus different angles of attack compared to Blade B. This could be due to a difference in the location of the section mass, elastic axis, or aerodynamic center locations in Blade A relative to Blade B. Perhaps the torsional stiffness of one blade is different from the other. We will continue to explore these effects and systematically run a series of parametric studies until we can focus on a most probable cause of both the 1P cyclic variation in the power and the wide difference in mean loads measured on Blades A and B. To date we have not chosen the most likely cause of this behavior.

CONCLUSIONS

In this paper we have described the steps we have taken to develop an analytical model of a very flexible rotor system using the ADAMS software. The Wind Eagle 300 Turbine, with its lightweight flexible rotor and hub was recently tested at the National Wind Technology Center. We have described progress to date in validating our analytical models of this machine.

We showed predicted results from both a "tuned" and "initial" model. We found that the "initial" model did a fairly good job of predicting the mean loads and power of this machine. At high wind speeds, this model overpredicted the mean power, possibly due to some error in modeling the correct amount of coupling between elastic flap motion and either elastic twist or rigid body pitch motion. The models also tended to underpredict the mean flap-wise bending moments for the higher wind speeds. Detailed measurements of the blade's coupled motions were not made in this study, and they are not planned in our future work, leaving some uncertainty as to the exact causes of these discrepancies. The discrepancy could also be due to the aerodynamic stall model.

We also developed a "tuned" model from the "initial" model by adjusting the tower stiffness values and the low-speed shaft torsional stiffness values in order to obtain more accurate prediction of the turbine's natural frequencies. In order to match the rotor's first symmetric flap natural frequency, we had to increase the damping in some of the joints, which connect the blade's root rib to the pitch control system and hub. Uncertainty in the amount of damping to apply to these joints is problematic for modeling this rotor system and remains an uncertainty. In comparing predictions from the "tuned" model to measured operating loads data, however, we found that the "tuned" model gave about the same results as the "initial" model over a range of wind speeds.

In addition, we observed two anomalies in the measured data, a large difference between the measured mean flap-wise and edge-wise bending

moments on Blade A versus Blade B, and a large 1P cyclic content in the measured shaft torque and power. These two anomalies are probably related. We have shown analytical model results from a "tuned" model in which we added a slight rotor mass imbalance to the model by shifting the center of gravity position of Blade A relative to Blade B. We saw that this "tuned" model with a mass imbalance provided a significant 1P cyclic variation in the predicted low-speed shaft torque, with closer agreement to the measured results.

We also showed results of incorporating another type of blade dissimilarity into the model, namely a difference in twist of one blade relative to the other. This type of dissimilarity not only increased the 1P contribution to the low-speed shaft torque, but also increased the difference in mean loads between the two blades. This machine exhibits a large difference in the mean loads between the two blades, which increases with wind speed.

We feel that these flexible turbines may be very sensitive to small differences in the blades, as we saw when we incorporated a small rotor mass imbalance into our model, or a difference in pitch or twist. Because such flexible machines undergo large deflections, and contain coupling between blade flap and twist motion, small differences in the blades may cause large differences in angles of attack, resulting in unwanted cyclic variations in the torque and power. We will continue to explore this hypothesis with further analyses.

The exact cause of these anomalies may never be fully discovered, since further in-depth testing of this machine is not currently planned. We can only explore possible causes of this behavior with our simulation codes.

FUTURE WORK

In the near future we plan to perform further detailed comparisons of code predictions with measured data and validate the models under turbulent wind inflow conditions. We also plan to perform further model parametric studies in order to find a most likely cause of the difference in mean loads between Blades A and B as well as explain the 1P cyclic variation in the low-speed shaft torque and machine power.

We then plan to finalize our model comparisons and write a final report on all of the model development and validation details.

ACKNOWLEDGMENTS

We thank the Cannon Energy Corporation and Dr. Jamie Chapman of OEM Development Corporation for the help and support they provided in this model development and validation effort. We also thank Dr. Kevin Jackson of Dynamic Design for his preparation of the turbine properties for our models. We wish to thank Dr. Gunjit Bir of NREL for his validation of the component models for this study. This work was supported by DOE under contract number DE-AC36-83CH10093.

REFERENCES

[1] Quarton, D.C. *Monitoring and Analysis of a Carter Wind Turbine*. Garrad Hassan & Partners Ltd, 1997. Report # ETSU W/24/00350/REP.

[2] Hansen, A.C. *User's Guide to the Wind Turbine Dynamics Computer Programs YawDyn and AeroDyn for ADAMS®, Version 10.0*. Salt Lake City, UT: University of Utah, January 1997. Prepared for the National Renewable Energy Laboratory under Subcontract No. XAF-4-14076-02.

[3] Wright, A.D., Kelley, N.D., Bir, G.S. *Analysis of a Two-bladed Flexible Rotor System: Model Development Progress.* Presented at the 36th AIAA Aerospace Sciences Meeting and Exhibit, Reno, NV, January 12-15, 1998.

[4] Dynamic Design. Flexible Turbine Model Description. August, 1997. Internal NREL report.

[5] Elliott, A.S., and Wright, A.D. *ADAMS/WT: An Industry-Specific Interactive Modeling Interface for Wind Turbine Analysis.* Wind Energy 1994, Edited by W.D. Musial, S.M. Hock, and D.E. Berg. SED-Vol. 14. New York: American Society of Mechanical Engineers; pp. 111-122, 23-26 January 1994.

[6] Kelley, N.D., Wright, A.D., and Osgood, R.M. "A Progress Report on the Characterization and Modeling of a Very Flexible Wind Turbine Design." To be presented at the 37th AIAA Aerospace Sciences Meeting and Exhibit, Reno, NV, January 1999.

[7] Buhl, M.L., Jr. *GPP User's Guide, A General-Purpose Postprocessor for Wind Turbine Data Analysis*. NREL/TP-442-7111. Golden, Colorado. National Renewable Energy Laboratory, 1995.

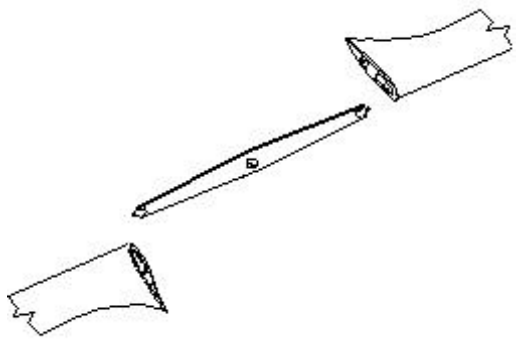

Figure 1. Illustration of the rotor system.

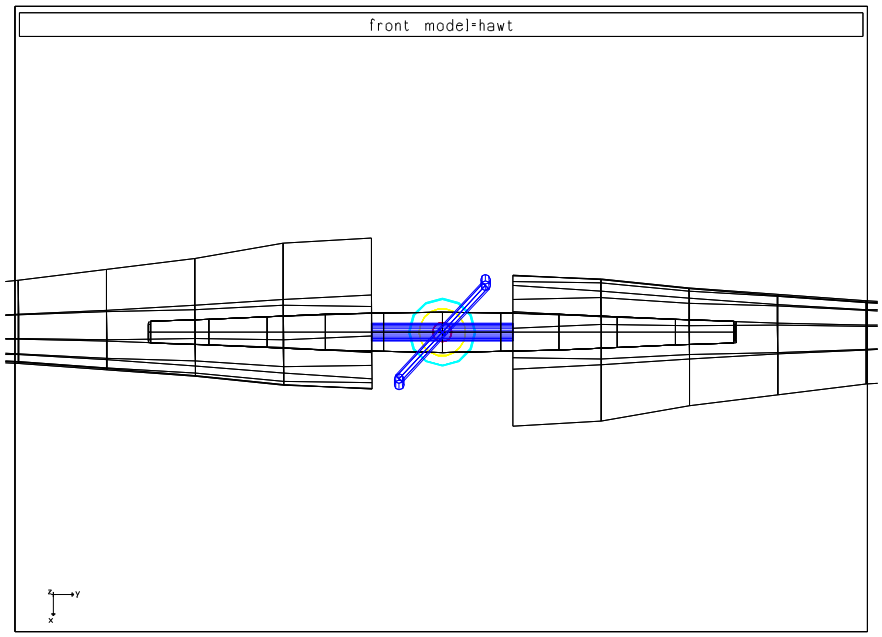

Figure 2. Illustration of the ADAMS rotor model.

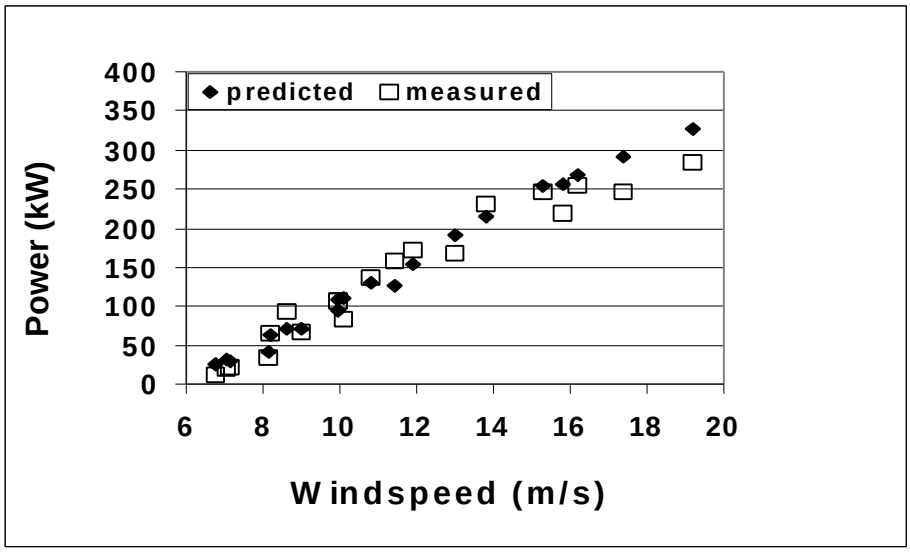

Figure 3. Comparison of Predicted and Measured Turbine Power.

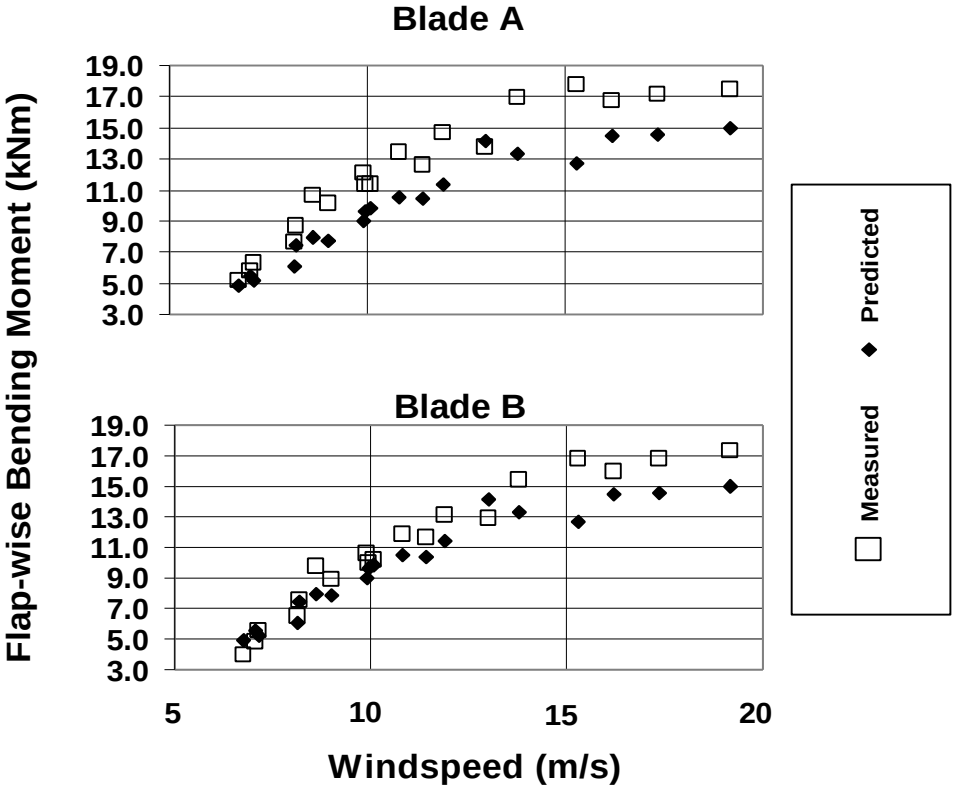

Figure 4. Comparison of Predicted and Measured Flexbeam Mean Flap-wise Bending Moments.

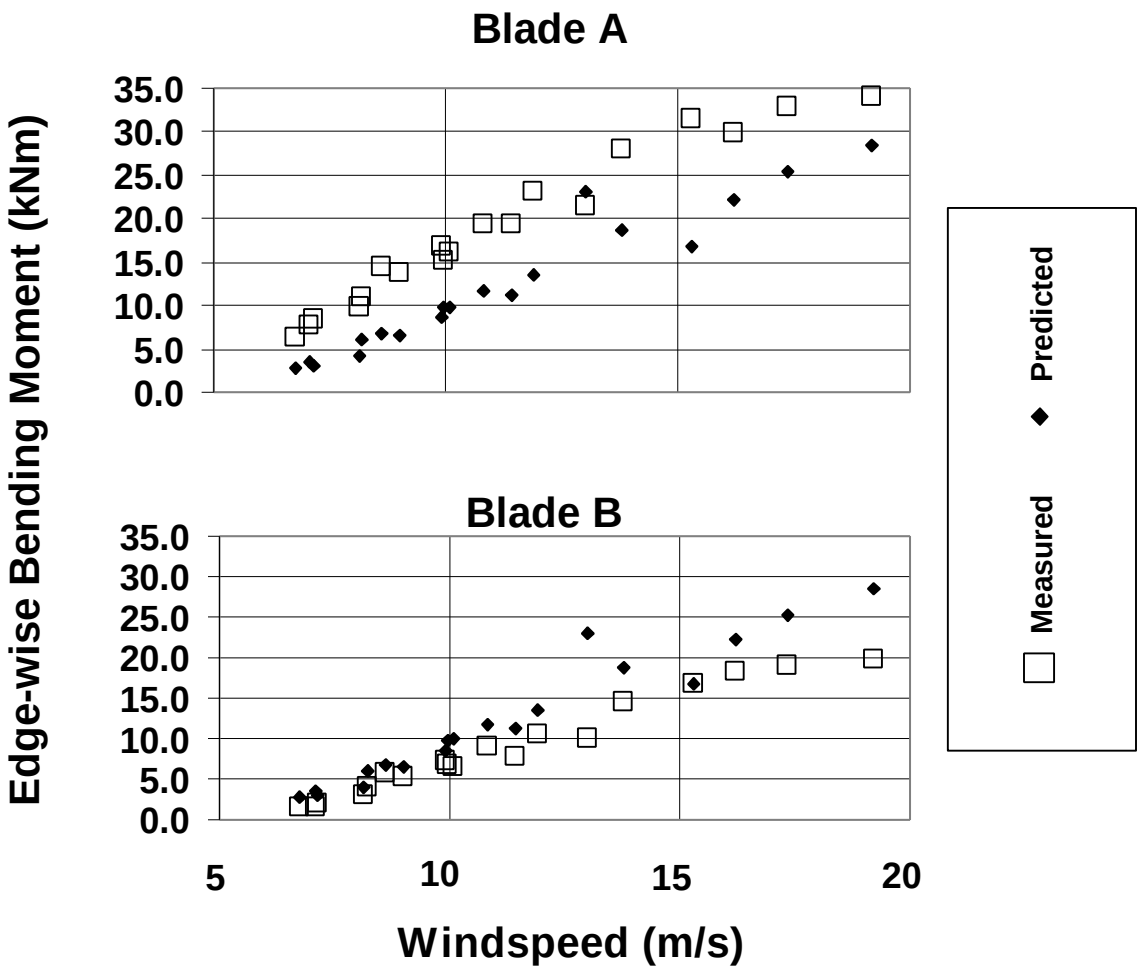

Figure 5. Comparison of Predicted and Measured Flexbeam Mean Edge-wise Bending Moment

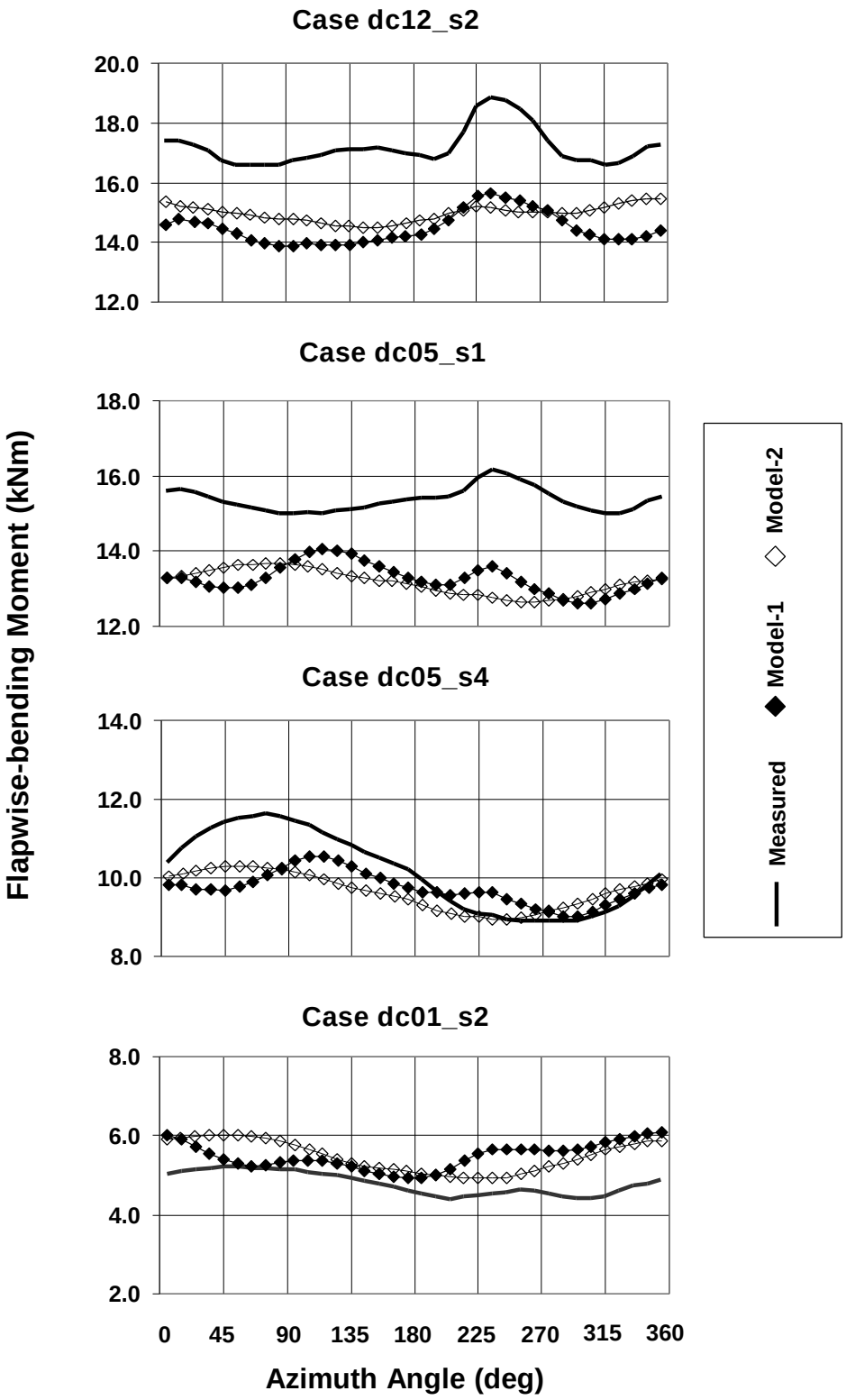

Figure 6. Plot of Azimuth Averaged Flexbeam Flapwise-bending Moments

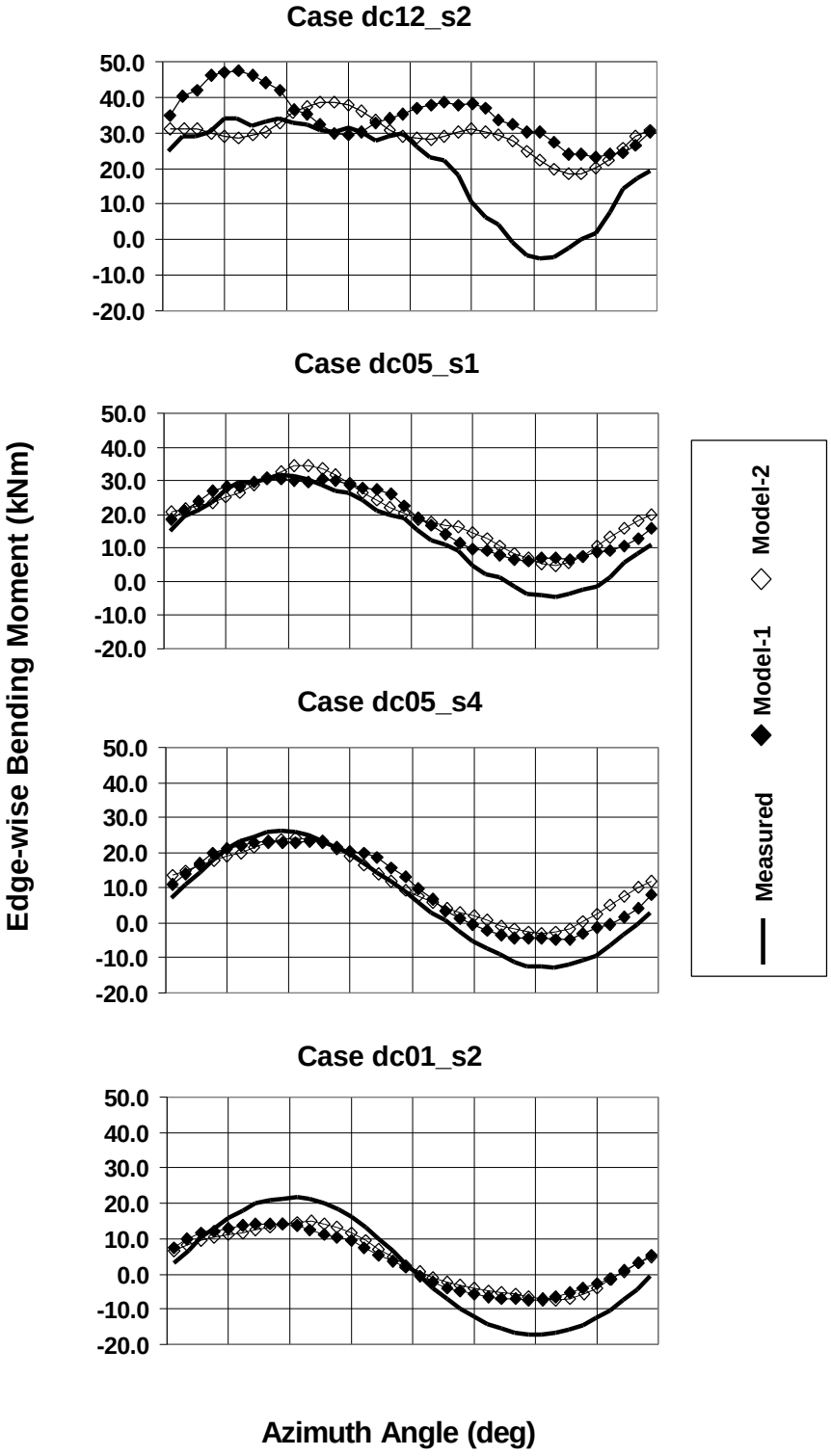

Figure 7. Plot of Azimuth Averaged Flexbeam Edgewise-bending Moments

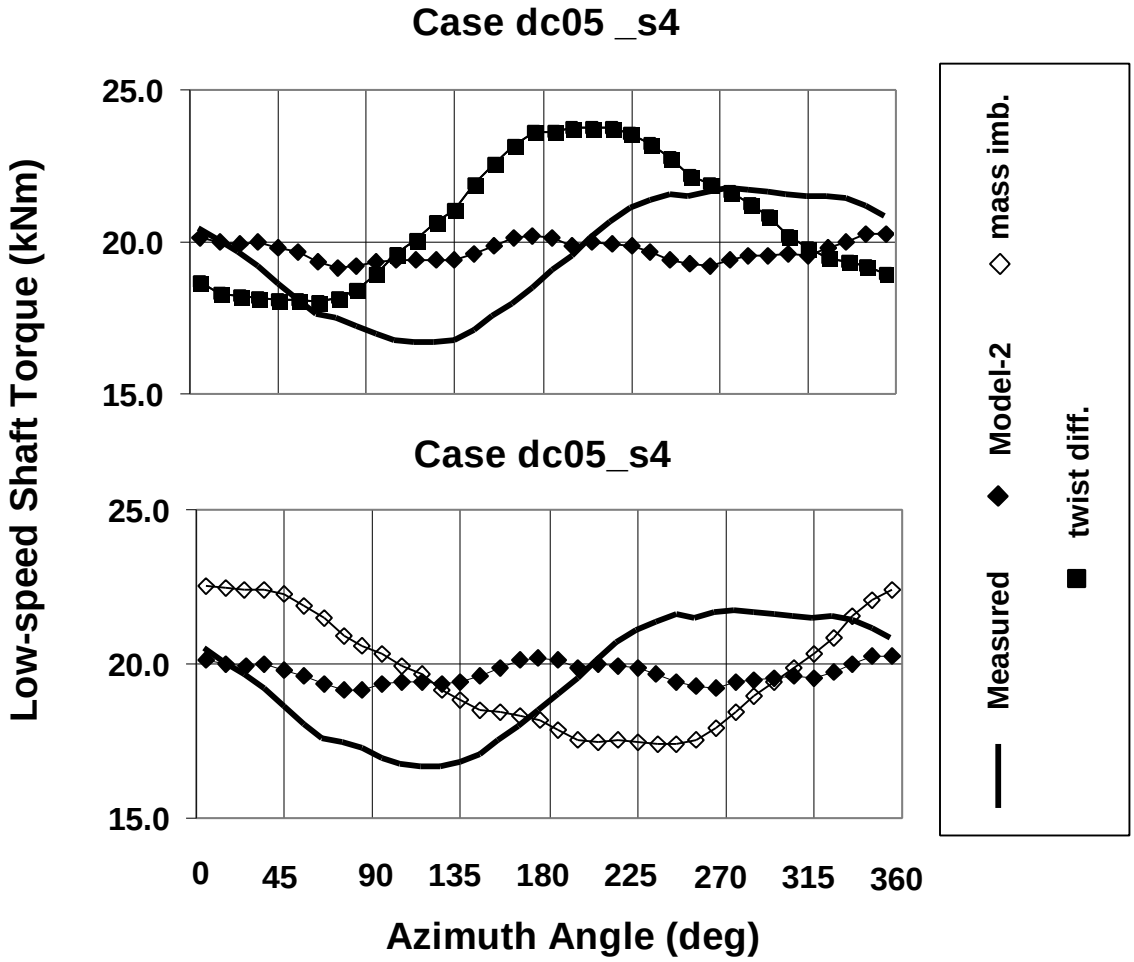

Figure 8. Plot of Azimuth Averaged Low-speed Shaft Torque.